Graphene oxide inhibits the lethal browning of *Cymbidium sinense* by reducing activities of enzymes.

Ting Wu[1], Juan Li[2], Jinglin Zhang[1], Minsong Lin[3], Zhimin Wu[1], Xiang Cai[1*], Weibin Xiang[4], Herong Guo[2], Shaozao Tan[3*], Zhisheng Zhang[2*]

[1]Department of Light Chemical Engineering, Guangdong Polytechnic, Lanshi, Chancheng, Foshan, China
[2]Guangdong Provincial Key Laboratory of Plant Molecular Breeding, South China Agricultural University, Wushan Road, Tianhe, Guangzhou, China
[3]Department of Chemistry, Jinan University, Huangpu Avenue (West), Tianhe, Guangzhou, China
[4]Scientific Research Office, Guangdong Polytechnic, Lanshi, Chancheng District, Foshan, China

Abstract

The major problems associated with plant tissue culture is browning of the culture medium, which invariably leads to decreased regenerative ability, poor growth and even death of the culture tissue. Here we show that the browning of *Chinese orchid* tissue culture was inhibited efficiently by graphene oxide. Our results demonstrate that the effect of the GO was much more effective than that of the activated charcoal (AC), resulting GO much more markedly promoted bud growth, reduced the browning index and alleviated the effect of browning during bud differentiation and development than AC. We found GO alleviated the browning by reducing the activities of enzymes like PPO and POD, and possibly by adsorbing quinones compounds. We anticipate our assay to be a starting point for more efficient plant tissue culture, and wildly used in agriculture, forestry, medicine, industry, and etc, producing a huge economic and social benefits.

Keywords: Graphene oxide, Tissue culture, Browning, Enzymes, *Chinese orchid*.

Accepted on February 23, 2018

Introduction

Tissue culture is an effective way of reproduction [1-4]. Under artificial conditions, organs, tissues, cells or protoplasts of plants are cultivated to obtain a complete regeneration. One of the major problems associated with plant tissue culture is serious browning, which invariably leads to decrease of regenerative ability, reduction of callus growth, inhibition of adventitious shoot formation and even death of the culture tissue [5,6]. Peroxidase (POD, EC 1.11.1.7) and polyphenol oxidase (PPO, EC 1.14.18.1) are the important enzymes in many plants. Their residual activity is detrimental to the quality of processed products of plants resulting in effects such as browning and loss of vitamins. Therefore, the inactivation of POD and PPO in the culture processing of plants is a major quality indicator of processed plants [5,6]. Activated charcoal (AC), [5] polyvinylpyrrolidone [7] and absorbic acid [8] are usually applied to control browning, however, these materials are not effectively to all the cultured plants, especially to the Chinese orchid [9].

Chinese orchid including of *Cymbidium sinense, Cymbidium goeringii, Cymbidium faberi, Cymbidium ensifolium and Cymbidium kanran*, is a popular terrestrial *Cymbidium* orchid which produces fragrant flowers and is often marketed as a high value potted specimen in eastern Asia [9]. So far, the studies and technologies of tissue culture of Chinese orchid have engendered limited achievements and applications due to the serious browning and slow growth of seedling during the differentiation process of rhizome [10].

Graphene oxide (GO), with a number of unique advantages as an inhibitor, such as large surface area to mass ratio, surface functionalities, good dispersion in aqueous solution or organic *solvents* and a fluctuant surface which could have induced-fit interaction with compounds containing benzene rings through π-π interaction, [11-13] has never been the subject of report relating to tissue culture of Chinese orchid. Here, we reported the first work that using GO as inhibitor, the browning of tissue culture of *Cymbidium sinense* cv.'XianDianBaiMo'(one of *Chinese orchid*) was inhibited efficiently.

GO was prepared by a two-step approach as illustrated in SI. The results in X-ray *diffraction*, Fourier Transform Infrared Spectroscopy and X-ray Photoelectron Spectrum (XPS) indicated the GO was successfully prepared. Figure 1a depicted a representative image of GO where GO was the silk-veil waves, and thin structure of the GO was also confirmed. The image in Figure 1b demonstrated the layered crystallites of GO with average inter-planar distance of about 0.935 nm, indicating that the chemical modification had a huge impact on the domain structure of the GO [14]. In Figure 1d, the XPS spectrum of GO showed four types of carbon bond: C-C (284.7 eV) of sp^2 carbon in the basal plane of GO, the carbon in C-O (286.9 eV), the carbonyl carbon in C=O (288.4 eV), and the carboxylate carbon in O-C=O (289.3 eV) [15,16]. The C/O At.% ratio of GO was 62/22. The Atomic Force Microscope (Figure 1c) demonstrated the thickness of GO was ca. 1.1 nm. In Raman spectrum, GO showed a two or three-layer structure. Under nitrogen atmosphere, the GO remained 43.7 % residue after heated to

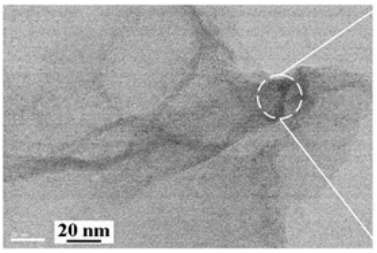

Figure 1a. *TEM image of GO.*

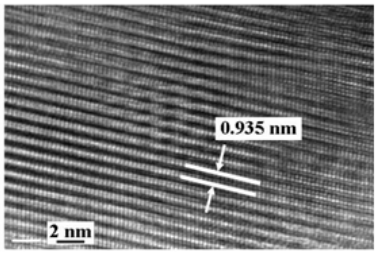

Figure 1b. *HRTEM image of GO with fringe spacing.*

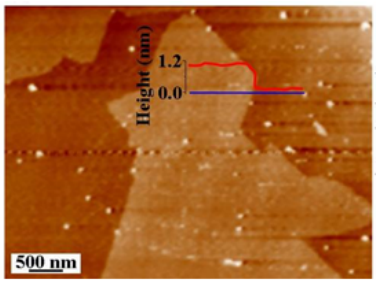

Figure 1c. *Tapping-mode AFM image of GO on a clean mica surface and cross-sectional profile of GO indicated by a blue line.*

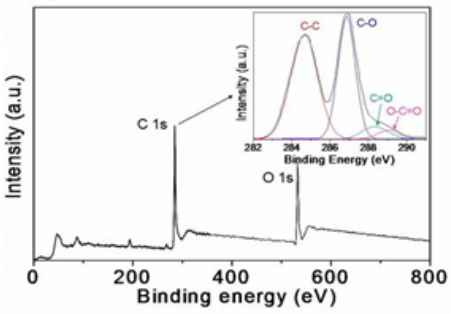

Figure 1d. *XPS profile of GO.*

700°C. The GO dispersion had a good colloidal stability, and a negative Zeta potential of -47.3 mV was found for GO in aqueous solution. The Brunauer-Emmett-Teller specific surface area of frozen dried GO was 467 m^2g^{-1}. Then, we displayed the GO markedly promoted bud growth, reduced the browning index and alleviated the effect of browning through outwardly observing the situations of bud differentiation and growth of rhizome of *Cymbidium sinense.*

As shown in Figure 2d, the difference of average number of bud differentiation between sample treated with 0.05 $mg{\cdot}mL^{-1}$ GO and blank control group (no addition of GO or AC) was not prominent ($P>0.05$), while the average number of bud differentiation of sample treated with 0.05 $mgmL^{-1}$ AC was significantly less than that of sample treated with 0.05 $mg{\cdot}mL^{-1}$ GO or blank control group ($P<0.01$). Besides, the bud growth of sample treated with 0.05 $mg{\cdot}mL^{-1}$ GO was better than that of sample treated with 0.05 $mg{\cdot}mL^{-1}$ AC or blank control group (Figures 2c and 2d). Such results indicated GO had no noteworthy influence on bud differentiation, but had positive effect on bud growth, and AC not only restrained the bud differentiation, but also hindered the bud growth.

On the other hand, Figure 2e showed the influence of GO on browning index of bud differentiation and growth process from rhizome of *Cymbidium sinense*. As seen, with the increase of incubation time, browning index of all the samples appeared a rising trend. After 6 days, the browning index of blank control group was significantly higher than that of sample treated with 0.05 $mg{\cdot}mL^{-1}$ GO or AC, and after 30 days, the browning index of sample treated with 0.05 $mg{\cdot}mL^{-1}$ GO was slightly higher than that of sample treated with 0.05 $mg{\cdot}mL^{-1}$ AC, showing GO or AC could dramatically decrease the browning index, and especially GO was more useful to prevent browning in early phase than AC, while AC had better effect for prevention of browning in later period of bud differentiation and growth than GO. In a way, such results demonstrated both GO and AC had the ability to effectively alleviate the browning during the process of differentiation and bud growth (Figures 2a and 2b).

As we know, the browning occurring in plant tissue culture is mainly caused by phenolic compounds that could undergo oxidation through polyphenol oxidase (PPO) and peroxidase (POD) to generate brown quinones compounds which have an inhibitory effect on the growth of plants, invariably leading to the death of plants [5,6]. Thus, the activities of enzymes like PPO and POD and the content of quinones compounds are the key factors during the browning process. In this regard, it was

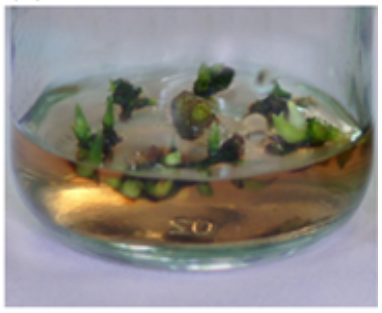

Figure 2a. *The pictures of bud differentiation and growth of Cymbidium sinense after culture for 30 days: blank control group, a bit big bud with light green color.*

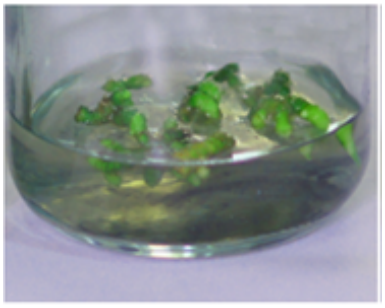

Figure 2b. *Supplement of 0.05 $mg{\cdot}mL^{-1}$ AC, small bud with light green color.*

important to investigate which factors mentioned above GO or AC had influence on.

First of all, we explored the changes of activities of PPO and POD with addition of 0.05 mg·mL^{-1} GO or AC during the process of differentiation and bud growth. As seen in Figures 3a and 3b, the addition of 0.05 mg·mL^{-1} GO could lower the activities of PPO and POD, while blank control group or sample treated with 0.05 mg·mL^{-1} AC had a rising trend for activities of PPO and POD. Moreover, the activities of PPO and POD of sample treated with GO were both memorably lower than those of blank control group and sample treated with 0.05 mg·mL^{-1} AC, indicating the effect of GO on prevention of browning was carried out by reducing the activities of PPO and POD. GO had a negatively charged surface because of the presences of active functionalities (Figure 1d), while PPO and POD had some positively charged points in their active centers [17-19]. Hence, in the incision of rhizome, inactivation of some active centers of PPO and POD was attributed to inter-attraction between GO and PPO and POD through electrostatic interaction, leading to reduction of activities of PPO and POD. Such result was similar with that in other study [20]. Conversely, although AC might also adsorb the PPO and POD in the incision of rhizome, the result showed it could hardly restrain the activities of PPO and POD. Therefore, we suggested because of simple capillary adsorption property, the effect of AC on prevention of browning was achieved by adsorbing the quinones compounds (Figures 3a and 3b).

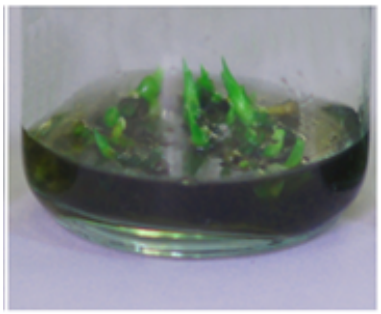

Figure 2c. *Supplement of 0.05 mg·mL^{-1} GO, big bud with deep green color.*

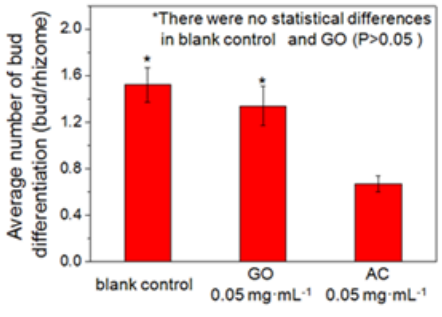

Figure 2d. *The average number of bud differentiation (bud/rhizome) after culture for 30 days.*

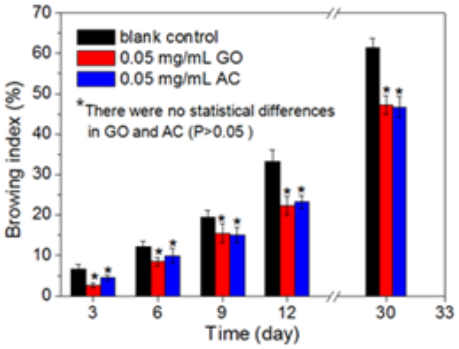

Figure 2e. *The browning index during the process of bud differentiation and growth. (means ± SD, n=7).*

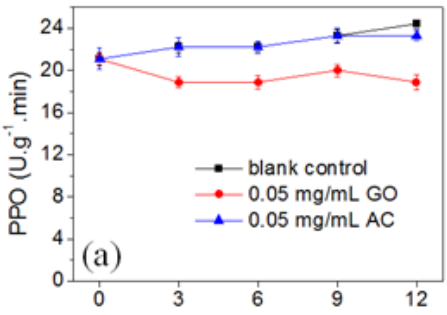

Figure 3a. *The changes of activities of PPO (a) and POD.*

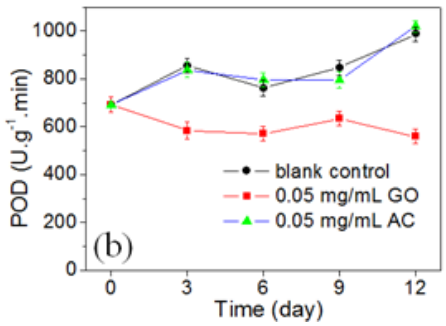

Figure 3b. *During the process of bud differentiation and growth (means ± SD, n=7).*

To further examine the hypothesis that the function of GO in alleviating browning was mainly realized by the decrease of activities of PPO and POD, resulting the decline of content of quinones compounds, while that of AC was only contributing to its non-specific adsorption effect, the adsorption properties of GO and AC as browning inhibitor were demonstrated by UV/Vis spectra, respectively. In Figure 3c, there was no absorption peak in UV/Vis spectrum of sample without rhizome and addition of GO or AC, indicating such sample released no quinones compounds in culture medium and auxins in culture medium had no absorption peak within wavelength range of 240 to 600 nm. Compared with other samples, the UV/Vis spectrum of blank control group (Figure 3c) showed a maximum absorption peak, suggesting it liberated most quinones compounds during the culture process. Compared with the two UV/Vis spectra (Figure 3c), the presences of absorption peaks were belonged to quinones compounds. The heights of absorption peaks of samples treated with 0.05 mg·mL^{-1} AC and GO were between the above two, indicating the reduction of content of quinones compounds, which proved the hypothesis mentioned above. To our surprise, more importantly, the height of the former was more than that of the latter, meaning the content of quinones compounds of sample treated with 0.05 mgmL^{-1} AC was more than that of sample treated with 0.05 mg·mL^{-1} GO. Thus, we made a conclusion that for inhibiting the browning, the mechanism of

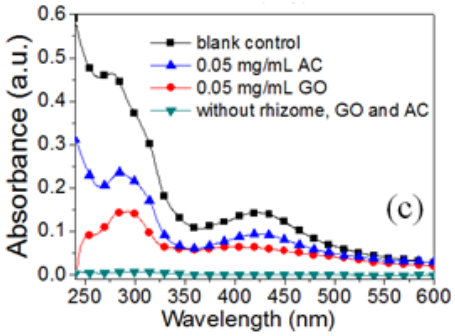

Figure 3c. *UV/Vis spectra of different culture mediums after culture for 30 days.*

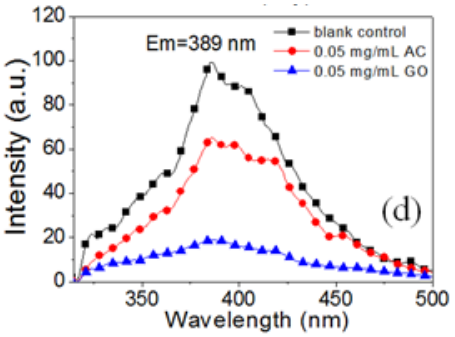

Figure 3d. *Fluorescence spectra of different culture mediums in aqueous solution (Ex=261 nm).*

GO was reduction of activities of enzymes like PPO and POD while that of AC was its simple capillary adsorption property, and effect of the former was much more effective than that of the latter, leading GO much more markedly promoted bud growth, reduced the browning index and alleviated the effect of browning during bud differentiation and development than AC.

Ulteriorly to confirm this conclusion, fluorescence spectra of quinones compounds upon no addition or addition of 0.05 $mg \cdot mL^{-1}$ GO and AC in aqueous solution were detected. Using blank control group, we confirmed the excitation wavelength and emission wavelength of quinones compounds were 261 nm and 389 nm, respectively. Fluorescence spectrum of blank control group showed a maximum emission peak (Figure 3d), meaning many quinones compounds were released during the culture process. The fluorescence quenching through addition of 0.05 $mg \cdot mL^{-1}$ AC was caused by reduction of content of quinones compounds, because AC adsorbed them through its capillary adsorption property. The fluorescence spectrum of sample treated with 0.05 $mg \cdot mL^{-1}$ GO was located in the lowest place, meaning the minimum content of quinones compounds was released in culture medium. The results of fluorescence spectra were consistent with those of UV/Vis spectra, and the conclusion mentioned above was proved again. Besides, the fluorescence quenching through addition of 0.05 $mg \cdot mL^{-1}$ GO might suggest that GO could also adsorb quinones compounds through π-π interaction, which had been revealed in our previous study [11]. In a conclusion, GO with such novel property was more importantly significant than AC in tissue culture.

In the end, far-UV Circular dichroism (CD) was used to compare the secondary structural change of AC or GO-treated POD and PPO. The activity of the enzyme is closely dependent on the structure of the enzyme, especially the active site. Many common conformational motifs containing α-helices, β-pleated sheets, poly-L-proline II-like helices and turns, have characteristic far UV (178-250 nm) CD spectra, and directly characterize the change of protein secondary conformation. It was observed that after pulsed electric fields treatment the secondary structure of POD and PPO was changed by CD analysis, which was related to the inactivation of enzymes [21,22]. Previously study also shown that GO can mimic as an artificial receptor and inhibit the activity of α-chymotrypsin, and GO exhibits the highest inhibition dose response (by weight) for α-chymotrypsin inhibition compared to all other reported artificial inhibitors [20].

It is commonly known that two negative peaks at 208 and 222 nm are characteristic of the α-helix secondary conformation of proteins, and that at 214 nm is characteristic of the β-sheet secondary conformation of proteins. The far UV CD spectra of all the samples were measured immediately after AC or GO treatment. The CD spectra of AC or GO-treated POD and PPO are illustrated in Figure 4. it was found that the CD spectrum change of GO-treated POD and PPO was more dramatic than that of AC-treated POD and PPO, testifying the above reasoning that GO was much more alleviating browning effective than AC to POD and PPO.

Figure 4a showed that POD itself has double negative peaks at around 208 and 222 nm in far UV CD spectra. After GO-treated the intensity of the two negative peaks in the CD spectra of POD decreased as compared with AC-treated, which indicated a loss of α-helix conformation of POD after GO-treated. According to the equation of α-helix fraction, the α-helix relative content of AC-treated POD were 99.76%, while the α-helix fraction of GO-treated POD was 94.28% (Figure 4b).

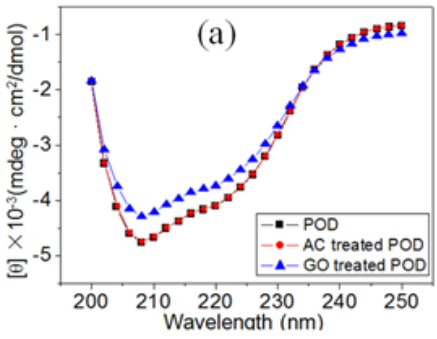

Figure 4a. *Far-UV CD spectra.*

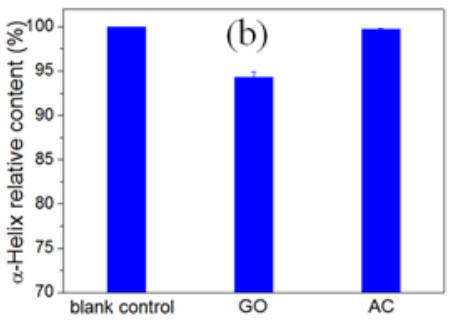

Figure 4b. *α-Helix relative content of AC or GO treated POD. POD concentration was 2.51 μM.*

The secondary structure of PPO was different from that of POD. Figure 4c showed that the CD spectra of PPO had two negative peaks at around 208 and 214 nm, indicating that it had β-sheets in its secondary structure besides α-helix. According to the equation of α-helix fraction, the α-helix relative content of AC-treated PPO and GO-treated PPO were 77.78% and 99.35%, respectively (Figure 4d).

In summary, we severally utilized AC and GO as browning inhibitor in tissue culture of Chinese orchid. The results showed that both AC and GO could alleviate the browning; however, the mechanisms and consequences of browning inhibition by AC and GO were entirely different. AC inhibited the browning through non-specific adsorption towards quinones compounds, leading the differentiation and bud growth had been negatively influenced. On the contrary, GO alleviated the browning by reducing the activities of enzymes like PPO and POD, and possibly by adsorbing quinones compounds. To our surprise, more importantly, the effect of the latter was much more effective than that of the former, resulting GO much more markedly promoted bud growth, reduced the browning index and alleviated the effect of browning during bud differentiation and development than AC. Given these advantages, we expected that the GO was a promising substance to preferably prevent browning and promote the growth of bud and seedling in plant tissue culture. We anticipate our assay to be a starting point for more efficient plant tissue culture system, and wildly used in agriculture, forestry, medicine, industry, and etc., producing a huge economic and social benefits.

Experimental Section

The details for the materials, preparation and characterization of the GO were described in the Supporting Information.

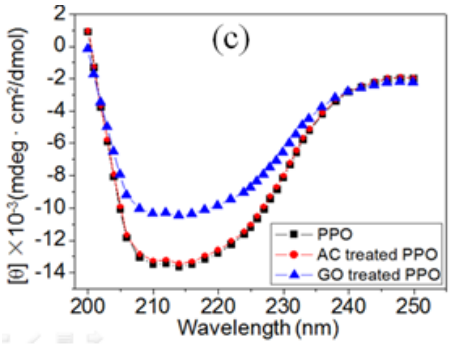

Figure 4c. *Far-UV CD spectra.*

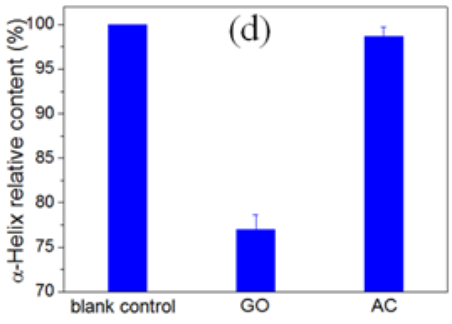

Figure 4d. *α-Helix relative content of AC or GO treated PPO. PPO concentration was 1.02 μM. (means ± SD, n=7).*

Materials

Rhizome cultured from the stem tip of Cymbidium sinense 'XianDianBaiMo', which was with good growth, consistent growth condition and identical subculture time, was used as the tissue culture material. Graphite powders (Spectral pure) were purchased from Sinopharm Chemical Reagent Co., Ltd and were used as received. Active charcoal and other reagents and solvents were obtained from commercial suppliers.

Peroxidase (from horseradish, 300 U/mg) and polyphenol oxidase (T7755, from mushroom, 2000 U/mg) from Sigma Co. (St. Louis, MO, USA). The molecular weight of POD and PPO was 44 and 128 kDa, respectively. Reaction substrates such as guaiacol, hydrogen peroxide and catechol were obtained from Beijing Chemicals Co. (Beijing, China). All chemicals used in the investigation were of analytical grade.

All aqueous solutions were prepared with ultrapure water (>18 MΩ) from a Milli-Q Plus system (Millipore).

Preparation of graphene oxide (GO)

GO was prepared by oxidizing natural graphite powder based on a modified Hummers method as originally presented by Kovtyukhova and colleagues [23,24]. As-prepared GO was dialyzed to remove residual salts and acids completely, and the resulting purified GO powder was collected by centrifugation and then air dried. GO powder was suspended in ultrapure water (0.5 mg•mL-1) and exfoliated through ultrasonication in a water bath (KQ218, 60 W) for 3 h, upon which the bulk GO powder was transformed into GO nanoplatelets. After that, the GO dispersion was obtained.

Characterization of GO

The as-produced GO was characterized by X-ray diffraction (XRD), Fourier Transform Infrared Spectroscopy (FTIR), Thermogravimetric Analysis (TGA), Ultraviolet–visible (UV/Vis), Raman Spectroscopy, Scanning Electron Microscope (SEM), Transmission Electron Microscope (TEM), X-ray Photoelectron Spectrum (XPS) and Atomic Force Microscope (AFM). The BET (Brunauer-Emmett-Teller) specific surface area and Zeta potential of GO were also tested.

General: XPS profile was recorded by an ESCALAB 250 X-ray Photoelectron Spectroscopy (Thermo-VG Scientific). TEM images were observed by using a JEOL JEM-2100F transmission electron microscope. AFM images were observed by an atomic force microscope (Benyuan CSPM5500) on a flat mica substrate. Zeta potential measurements were performed using a Zetasizer nano ZS (Malvern Instruments). UV/Vis spectra were recorded by a Hitachi 330 UV-Vis spectrophotometer. XRD patterns were taken by a Rigaku D/max 2500v/pc X-ray diffractometer using Cu Kα radiation (Kα=0.15405 nm) at a scanning rate of 10.0 °/min, using a voltage of 40 kV and a current of 200 mA. FTIR spectra were obtained on a Nicolet 6700 spectrometer. BET specific surface area was determined using Micromeritics ASAP 2010 instrument. Fluorescence spectra were detected by a Hitachi F4600 fluorescence spectrophotometer. Raman spectra were obtained with a Renishaw INVIA spectrometer, and the 514.5 nm radiation from a 20 mW air-cooled argon ion laser was used as the excitation source. Thermogravimetric

analysis (TGA) was conducted with a thermal analyzer (SDT-Q600). SEM images were observed by using a PHILIPS XL-30 scanning electron microscopy.

Culture of material

The rhizome was chopped in pieces with length of about 1.0 cm, and then inoculated in culture flasks containing different culture mediums (1/2 Murashige and Skoog medium + 3.0 mg·L^{-1} 6-benzyladenine + 0.5 mg·L^{-1} α-naphthalene acetc acid + 30 g·L^{-1} sugarcane + 7.0 g·L^{-1} carrageenan + 0.1 g·L^{-1} phaseomannite + 0.05 mg·mL^{-1} GO or 1/2 Murashige and Skoog medium + 3.0 mg·L^{-1} 6-benzyladenine + 0.5 mg·L^{-1}α-naphthalene acetc acid + 30 g·L^{-1} sugarcane + 7.0 g·L^{-1} carrageenan + 0.1 g·L^{-1} phaseomannite + 0.05 mg·mL^{-1} AC). After that, the rhizomes were cultured in culture room at (25±2)°C under illumination with intensity of (1000±200) lx for 12 h·d^{-1}. Each culture flask had 8 pieces of rhizomes and 6 culture flasks were regarded as a repetition. The experiment was repeated four times.

Observations of differentiation and bud growth and browning

Situations of differentiation and bud growth and browning were respectively observed every 3 d during the culture process. The degree of browning was recorded according to: level 0, no browning; level 1, browning only occurred in the incision of explant; level 2, browning appeared in culture medium with area of less than 0.5 cm^2 where the explant was the center; level 3, browning arose in culture medium with area of more than 0.5 cm^2 where the explant was the center. Besides, the number of bud differentiation was also recorded after culture for 30 d. Then, the average number of bud differentiation and browning index were calculated in accordance with equations (1) and (2), respectively.

$$\text{The average number of bud differentiation (bud/rhizome)} = \frac{\text{Total number of differentiated bud}}{\text{Total number of inoculated rhizome}} \quad (1)$$

$$\text{Browning index} = \frac{\sum(\text{The number of explant}) \times (\text{Corresponding level of browning})}{(\text{Total number of explant}) \times (\text{The highest level of browning})} \times 100\,\% \quad (2)$$

Crude extract of polyphenol oxidase (PPO) and peroxidase (POD)

The general protocol for extract and assay of activity of PPO and POD referred to Du et al. [21]. In brief, after elimination of the surface solid particles, freshed samples of rhizomes which had been respectively cultured for 3 d, 6 d, 9 d and 12 d were preserved in triplicate in refrigerator at -20°C and were standby. Then, 0.1 g of frozen sample was grinded in 0.1 mol·L^{-1} of buffer solution of potassium phosphate (pH=7.0, 1.0 % of polyvinyl pyrrolidone) to obtain homogenate. The homogenate was orderly centrifuged for 30 min at 12000 rpm and for 15 min with centrifugal force of 6000 ×g to get supernatant which was the crude extract of PPO and POD.

Assay of activity of PPO in rhizome

2.9 mL of buffer solution of potassium phosphate (0.1 mol·L^{-1}) and 1 mL of catechol (0.1 mol·L^{-1}) were mixed in water bath at 37°C. After 0.1 mL of the crude extract of enzymes was added, the solution was stirred rapidly and uniformly, and then it was immediately monitored by measuring its optical density (O.D) at 525 nm which was designated as $O.D_1$. After reaction for 3 min, the O.D of solution which was designated as $O.D_2$ was measured again. The zero adjustment was carried out by replacing crude extract of enzymes with buffer solution of potassium phosphate. The expression of enzymatic activity is using the change of enzyme unit (U) of per gram of plant material in unit time (min), which is expressed as U/(g·min). One enzyme unit (U) indicates the change of 0.01 of O.D. The activity of PPO is calculated according to the eqn. (3).

$$\text{Activity of PPO} = \frac{(O.D_1 - O.D_2)}{(0.01 \times \frac{W}{V_1} \times V_2 \times \min)} \quad (3)$$

Assay of activity of POD in rhizome

1.8 mL of buffer solution of potassium phosphate (0.1 mol·L^{-1}), 2 mL of hydrogen dioxide solution (24 mmol·L^{-1}) and 0.1 mL of guaiacol (8 mmol·L^{-1}) were mixed in water bath at 37°C. After 0.1 mL of the crude extract of enzymes was added, the solution was stirred rapidly and uniformly, and then it was immediately monitored by measuring its optical density (O.D) at 470 nm which was designated as $O.D_1$. After reaction for 3 min, the O.D of solution which was designated as $O.D_2$ was measured again. The zero adjustment was carried out by replacing crude extract of enzymes with buffer solution of potassium phosphate. The expression of enzymatic activity is using the change of enzyme unit (U) of per gram of plant material in unit time (min), which is expressed as U/(g·min). One enzyme unit (U) indicates the change of 0.01 of O.D. The activity of POD is calculated according to the eqn. (4).

$$\text{Activity of POD} = \frac{(O.D_1 - O.D_2)}{(0.01 \times \frac{W}{V_1} \times V_2 \times \min)} \quad (4)$$

UV/Vis spectra and fluorescence spectra analysis

Culture mediums (after culture for 30 days) were transformed from solid state to liquid state using heating at 40-50°C. 2 mL culture medium was diluted with 8 mL deionized water to form homogeneous solution. Then, the solution was used for analysis without further processing.

AC or GO treated PPO

The AC or GO treated POD activity was assayed by using hydrogen peroxide and guaiacol as the reaction substrates. The reaction medium contained 7 μL of 30% hydrogen peroxide and 28 μL of liquid guaiacol in 100 ml of 0.1 M acetate buffer, pH 5.6. POD concentration was 0.025 μM, and AC or GO concentration was 0.05 mg·mL^{-1}. The AC or GO treated POD activity was determined by adding 0.1 ml of POD to 5.9 ml substrate solution. The mixed solution was allowed at 30°C for 12 h.

AC or GO treated POD

The AC or GO treated POD activity was assayed with catechol as a substrate. The reaction mixture included 2 mL of 0.1 M catechol and 1 mL of 0.1 M phosphate buffer at pH 6.8 which

were incubated at 37°C. Then 2.0 mL of 0.0133 μM (3.4 U/ml) POD solution (AC or GO concentration was 0.05 mg·mL^{-1}) was added to the reaction mixture to initiate the enzyme reaction. The mixed solution was allowed at 37°C for 12 h.

Circular dichroism (CD) analysis

CD spectra were recorded with a JASCO 810 CD spectropolarimeter (Japan Spectroscopic Company, Tokyo, Japan), using quartz cuvette of 1 mm optical path length at room temperature (25 ± 1°C). CD spectra were scanned at the far UV range (250-200 nm) with four replicates at 50 nm/min. The CD data was expressed in terms of mean residual ellipticity, (θ), in deg cm^2 dmol^{-1}.

$$\alpha\text{-Helix relative content} = \frac{\text{content of } \alpha\text{-helix after treatments}}{\text{content of } \alpha\text{-helix before treatments}} \times 100\% \quad (5)$$

$$\alpha\text{-helix} = \frac{(\theta) + 4000}{29000} \quad (6)$$

Statistical analysis

Statistical analysis was performed using Statistical Product and Service Solutions software statistical software (SPSS 11.0, United States). The differences between the groups were assessed using the analysis of variance test. The results were considered statistically significant when the P value was <0.01.

Results and Discussion

Synthesis of GO

The synthesis of GO: step 1, oxidative treatment of graphite yielded multi-layer GO; step 2, the ultrasonic treatment of multi-layer GO produced a water-soluble and few-layer GO dispersion (Figure 5).

X-ray diffraction (XRD) patterns

XRD patterns were taken by a Rigaku D/max 2500v/pc X-ray diffractometer using Cu Kα radiation (Kα=0.15405 nm) at a scanning rate of 10.0 °/min, using a voltage of 40 kV and a current of 200 mA (Figure 6).

The low XRD signal-to-noise ratios of GO was attributed to the poor crystallinity of the sample. For graphite, the sharp and intensive peak at 2θ=26.4º indicated a highly organized crystal structure with the (002) interlayer spacing of 0.337 nm. For GO, the peak at 2θ=26.4º could not be observed, and a new peak centered at 2θ=9.45º, corresponding to the (002) interlayer spacing of 0.935 nm, which might be due to high degree of exfoliation and disordered structure of GO. Similar results had been observed by other XRD studies [25,26].

Fourier Transform Infrared Spectroscopy (FTIR) spectra

FTIR spectra were obtained on a Nicolet 6700 spectrometer.

Figure 7 showed FTIR spectra of graphite and GO. As observed from FTIR spectrum of GO, the very broad and intensive peak appeared at 3430 cm^{-1} was assigned to O-H stretching band, which might originate from water adsorbed inside GO. Peaks at 1726 cm^{-1}, 1622 cm^{-1}, 1385 cm^{-1}, and 1052 cm^{-1} were corresponded to C=O, C-OH, C=C, and C-O-C vibration frequency, respectively. Compared with those of pristine graphite, these new peaks suggested that graphite had been successfully oxidized to generate GO [27,28].

Thermogravimetric Analysis (TGA) curve

TGA curve was conducted with a thermal analyzer (SDT-Q600),

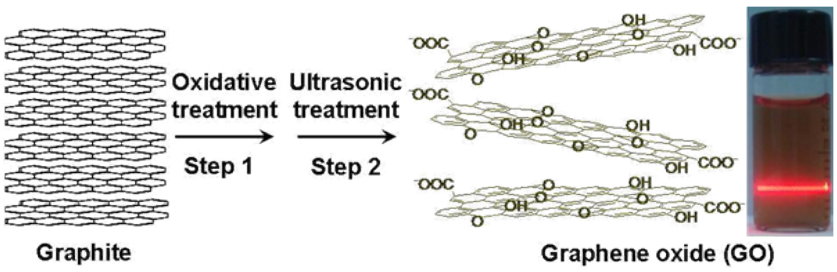

Figure 5. *The synthesis of GO: step 1, oxidative treatment of graphite yielded multi-layer GO; step 2, the ultrasonic treatment of multi-layer GO produced a water-soluble and few-layer GO dispersion.*

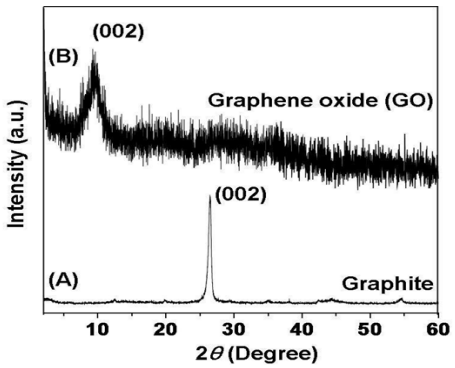

Figure 6. *XRD patterns of (A) graphite; (B) GO.*

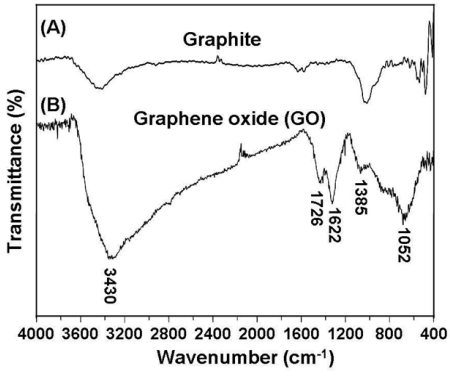

Figure 7. *FTIR spectra of (A) graphite; (B) GO FTIR spectra were obtained on a Nicolet 6700 spectrometer.*

and samples were heated from 40°C to 800°C under N2 flow at a scanning rate of 10°C/min (Figure 8).

Ultraviolet–visible (UV/Vis) spectrum

The inset of UV/Vis spectrum in Figure 9 showed GO exhibited a typical maximum absorption at 233 nm. Figure 9 showed the change of relative absorbance with respect to the setting time for GO. It was found that there was little change in relative absorbance for GO samples, which proved the resultant GO dispersion had a good colloidal stability.

Moreover, after 14 d standing, the GO dispersion showed Tyndall effect, demonstrating that GO dispersion had a good colloidal stability as well.

BET specific surface area and Zeta potential

Zeta potential measurements were performed using a zeta sizer nano ZS (Malvern Instruments), and all the aqueous samples were diluted to 0.05 mg•mL-1 before measurements. BET (Brunauer-Emmett-Teller) specific surface area was determined using Micromeritics ASAP 2010 instrument (Figure 10).

The stability of GO in aqueous solution through electrostatic repulsion was characterized by Zeta potential [29,30]. A negative zeta potential of -47.3 mV was found for GO in aqueous solution at a concentration around 0.05 mgmL^{-1} (pH 7, prepared by diluting the purified GO in ultrapure water). According to the definition of colloid stability with zeta potential by the ASTM (American Society for Testing and Materials) Standard D4187-82 (ASTM Standard D4187-82 1985), the GO dispersion in the aqueous solution had ‘‘good stability’’ with zeta potential values among ±40 to ±60 mV [22]. The good stability of the GO dispersion was due to the aqueous solubility imparted by the carboxyl groups of GO and the fact that the intermolecular electrostatic repulsion of these functional groups had prevented the aggregation.

The BET specific surface area of frozen dried GO was 467 m2•g-1.

Raman spectrum

Raman spectra were obtained with a Renishaw inVia spectrometer, and the 514.5 nm radiation from a 20 mW air-cooled argon ion laser was used as the excitation source.

In Raman spectrum (Figure 11), GO displayed two prominent peaks at 1600 and 1354 cm^{-1}, which were corresponded to the G and D bands, respectively. Meanwhile, there was a small peak named G’ or 2D band at about 2600-2700 cm^{-1}, which could be used to calculate the number of layers for GO. From the result shown in the insert of Figure 11, it was found that GO showed a two or three-layer structure [31,32].

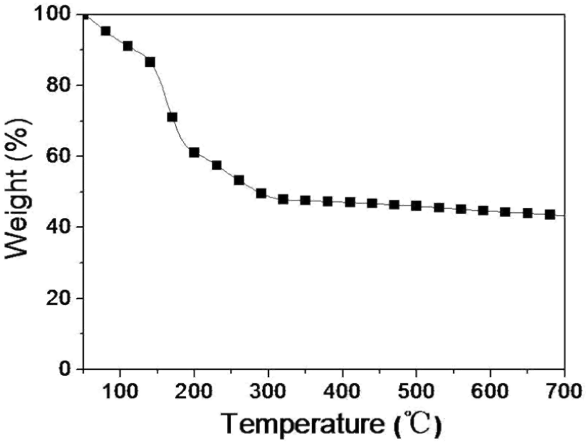

Figure 8. *TGA curve of GO.*

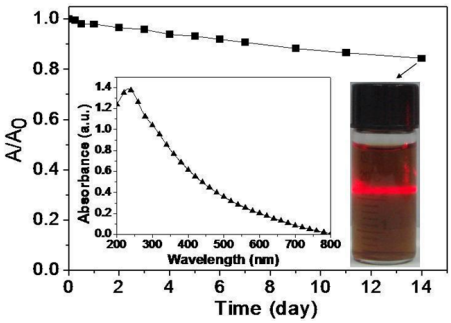

Figure 9. *The change of relative absorbance with respect to the setting time for GO in aqueous solution at 233 nm (the inset of UV/Vis spectrum showed the absorption spectra of 0.05 mg·mL^{-1} GO in aqueous solution, and the inset picture showed the image of 0.05 mg·mL^{-1} GO after 14 d standing).*

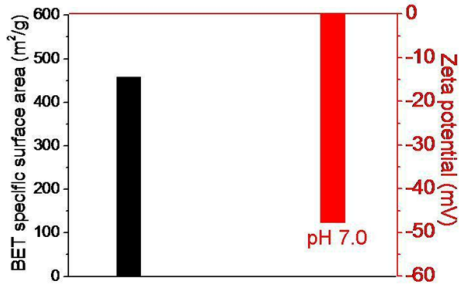

Figure 10*. The BET specific surface area and Zeta potential of GO.*

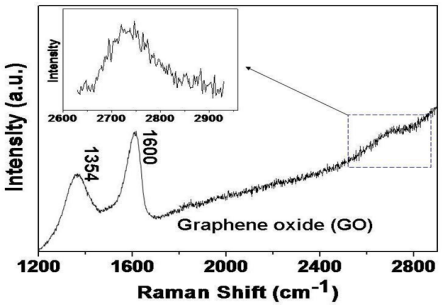

Figure 11. *Raman spectrum of GO (radiation at 514.5 nm).*

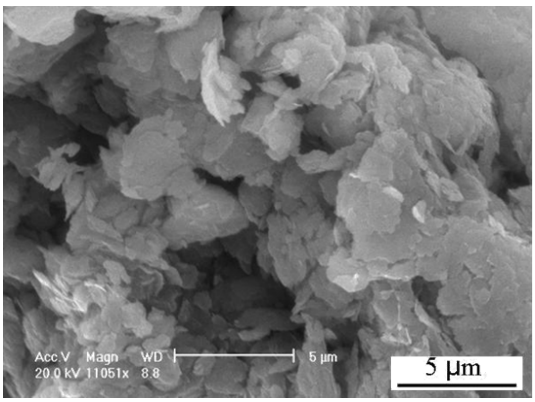

Figure 12. *SEM image of GO.*

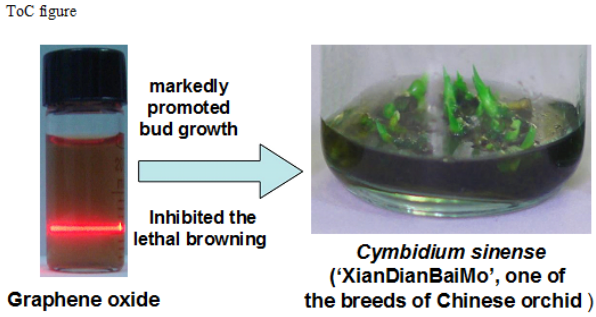

Figure 13. *Graphene oxide inhibits the lethal browning.*

Scanning Electron Microscope (SEM) image

The morphology of the GO was observed by SEM using PHILIPS XL-30 scanning electron microscopy. In the SEM image (Figures 12 and 13), GO appeared to be piled up with thick scales, which implied that the GO prepared in the present study had a scale-like structure. Similar results had been obtained in other studies [33].

Conclusion

Graphene Oxide (GO) was prepared by modified Hummers method and characterized by different techniques like X-ray diffraction, Fourier Transform Infrared Spectroscopy, Thermogravimetric Analysis, Ultraviolet–visible, Raman Spectroscopy, Scanning Electron Microscope, Transmission Electron Microscope, X-ray Photoelectron Spectrum and Atomic Force Microscope. Analysis of these characterizations showed the presence of GO in the prepared sample. Go was then used in the culture medium of *Chinese orchid* tissue culture, which inhibited the browning effect by reducing the browning index and promoted bud growth.

Acknowledgements

This work was financially supported by the National Natural Science Foundation of China (21476052), the Foundation of Science and Technology Projects of Guangdong Province (No. 2016A010103047), Foshan modern dyeing and finishing technology research center (2016GA10161) the Science and technology innovation platform project of Foshan City (2016AG100541, 2015AG10020), the Talent Introduction Project of Guangdong Polytechnic (K2015002).

References

1. Rout GR, Mohapatra A, Jain SM. Tissue culture of ornamental pot plant: A critical review on present scenario and future prospects. Biotechnology Advances. 2006;24(6):531-60.
2. Pischke MS, Huttlin EL, Hegeman AD, et al. A transcriptome-based characterization of habituation in plant tissue culture. Plant Physiology. 2006;140(4):1255-78.
3. Doran PM. Foreign protein degradation and instability in plants and plant tissue cultures. Trends in Biotechnology. 2006;24(9):426-32.
4. Misra P, Toppo DD, Gupta N, et al. Effect of antioxidants and associate changes in antioxidant enzymes in controlling browning and necrosis of proliferating shoots of elite Jatropha curcas L. Biomass and Bioenergy. 2010;34(12):1861-9.
5. Thomas TD. The role of activated charcoal in plant tissue culture. Biotechnology Advances. 2008;26(6):618-31.
6. Tang W, Newton RJ. Increase of polyphenol oxidase and decrease of polyamines correlate with tissue browning in Virginia pine (Pinus virginiana Mill.). Plant Science. 2004;167(3):621-8.
7. Huang LC, Lee YL, Huang BL, et al. High polyphenol oxidase activity and low titratable acidity as causes of browning of bamboo tissue culture in vitro, and basic characteristics of the enzyme. In Vitro Cell. Dev. Biol-Plant. 2002;38:358-65.
8. Ko WH, Su CC, Chen CL, et al. Control of lethal browning of tissue culture plantlets of Cavendish banana cv. Formosana with ascorbic acid. Plant Cell, Tissue and Organ Culture (PCTOC). 2009; 96(2):137-41.
9. Chang C, Chang WC, et al. Effect of thidiazuron on bud development of Cymbidium sinense Willd in vitro. Plant Growth Regulation. 2000;30(2):171-5.
10. Wu T, Cai X, Tan S, et al. Adsorption characteristics of acrylonitrile, p-toluenesulfonic acid, 1-naphthalenesulfonic acid and methyl blue on graphene in aqueous solutions. Chemical Engineering Journal. 2011;173(1):144-9.
11. Cai X, Tan S, Lin M, et al. Synergistic antibacterial brilliant blue/reduced graphene oxide/quaternary phosphonium salt composite with excellent water solubility and specific targeting capability. Langmuir. 2011;27(12):7828-35.
12. Cai X, Tan S, Yu A, et al. Sodium 1□Naphthalenesulfonate□ Functionalized Reduced Graphene Oxide Stabilizes Silver Nanoparticles with Lower Cytotoxicity and Long□Term Antibacterial Activity. Chemistry-An Asian Journal. 2012;7(7):1664-70.
13. Zhang X, Feng Y, Huang D, et al. Investigation of optical modulated conductance effects based on a graphene oxide–azobenzene hybrid. Carbon. 2010;48(11):3236-41.
14. Cai X, Tan S, Xie A, et al. Conductive methyl blue-functionalized reduced graphene oxide with excellent stability and solubility in water. Materials Research Bulletin. 2011;46(12):2353-8.
15. Cai X, Lin M, Tan S, et al. The use of polyethyleneimine-modified reduced graphene oxide as a substrate for silver nanoparticles to produce a material with lower cytotoxicity and long-term antibacterial activity. Carbon. 2012;50(10):3407-15.
16. Queiroz C, Mendes ML, Fialho E, et al. Polyphenol oxidase: characteristics and mechanisms of browning control. Food reviews international. 2008;24(4):361-75.
17. Choi HJ, Kang SW, Yang CH, et al. Crystal structure of a novel human peroxidase enzyme at 2.0 Å resolution. Nature Structural and Molecular Biology. 1998;5(5):400.

18. Zhu H, Srivastava R, McShane MJ. Spontaneous loading of positively charged macromolecules into alginate-templated polyelectrolyte multilayer microcapsules. Biomacromolecules. 2005;6(4):2221-8.
19. De M, Chou SS, Dravid VP. Graphene oxide as an enzyme inhibitor: modulation of activity of α-chymotrypsin. Journal of the American Chemical Society. 2011;133(44):17524-7.
20. Zhong K, Wu J, Wang Z, et al. Inactivation kinetics and secondary structural change of PEF-treated POD and PPO. Food Chemistry. 2007;100(1):115-23.
21. Du BG, Nian H, Zhang ZS, et al. Effects of aluminum on superoxide dismutase and peroxidase activities, and lipid peroxidation in the roots and calluses of soybeans differing in aluminum tolerance. Acta Physiol. Plant. 2010;32:883-90.
22. Standard ASTM. Zeta potential of Colloids in Water and Waste Water. American Society for Testing and Materials. 1985;pp:4182-7.
23. Kovtyukhova NI, Ollivier PJ, Martin BR, et al. Layer-by-Layer assembly of ultrathin composite films from micron-sized graphite oxide sheets and polycations. Chem Mater. 1999; 11:771-8.
24. Hummers WS, Offeman RE. Preparation of graphitic oxide. J Am Chem Soc. 1958;80:1339.
25. Cai X, Lin M, Tan S, et al. The use of polyethyleneimine-modified reduced graphene oxide as a substrate for silver nanoparticles to produce a material with lower cytotoxicity and long-term antibacterial activity. Carbon. 2012;50:3407-15.
26. Cai X, Tan S, Yu A, et al. Sodium 1-naphthalenesulfonate-functionalized reduced graphene oxide stabilizes silver nanoparticles with lower cytotoxicity and long-term antibacterial activity. Chem-Asian J. 2012;7:1664-70.
27. Jeong HK, Lee YP, Lahaye RJWE, et al. Evidence of graphitic AB stacking order of graphite oxides. J Am Chem Soc. 2008;130:1362-6.
28. Guo HL, Wang XF, Qian QY, et al. A green approach to the synthesis of graphene nanosheets. ACS Nano. 2009;3:2653-59.
29. Vichchulada P, Zhang Q, Duncan A, et al. Macroscopic electrical properties of ordered single-walled carbon nanotube networks. ACS Appl Mater Interfaces. 2010;2:467-73.
30. Si Y, Samulski ET. Synthesis of water soluble graphene. Nano Lett. 2008;8:1679-82.
31. Eda G, Fanchini G, Chhowalla M. Large-area ultrathin films of reduced graphene oxide as a transparent and flexible electronic material. Nat Nanotechnol. 2008;3:270-4.
32. Ferrari AC, Meyer JC, Scardaci V, et al. Raman spectrum of graphene and graphene layers. Phys Rev Lett. 2006;97:187401.
33. Wu T, Cai X, Tan S, et al. Adsorption characteristics of acrylonitrile, p-toluenesulfonic acid, 1-naphthalenesulfonic acid and methyl blue on graphene in aqueous solutions. Chem Eng J. 2011;173:144-9.

***Correspondence to:**

Xiang Cai
Professor
Department of Light Chemical Engineering
Guangdong Polytechnic
Chancheng District
Foshan, Guangdong
China
Tel: +86 0757 83106906
E-mail: cecaixiang@163.com

Zhisheng Zhang
Professor
Guangdong Provincial Key Laboratory of Plant Molecular Breeding
South China Agricultural University
No. 483, Wushan Road
Tianhe District, Guangzhou
China
Tel: +86 020 38297154
E-mail: zszhang@scau.edu.cn

Shaozao Tan
Professor
Department of Chemistry
Jinan University
No. 601, Huangpu Avenue (West)
Tianhe District, Guangzhou
China
Tel: +86 020 85223670
E-mail: tanshaozao@163.com